C3G shows regulated nucleocytoplasmic exchange and represses histone modifications associated with euchromatin

Dhruv Kumar Shakyawar, Kunal Dayma, Anesh Ramadhas, Chavvakula Varalakshmi, and Vegesna Radha*
Centre for Cellular and Molecular Biology, Hyderabad 500 007, India

ABSTRACT **C3G (RapGEF1) is a ubiquitously expressed guanine nucleotide exchange factor that functions in signaling pathways regulating cell proliferation, apoptosis, and actin reorganization. It is essential for differentiation and early embryonic development in mice. Overexpressed C3G shows predominant cytoplasmic localization, but endogenous C3G is a component of nuclear fractions in a variety of cell types. Coexpression of importin-α and inhibition of nuclear export by leptomycin B resulted in predominant nuclear localization of C3G. Functional NLSs, NES, and GSK3-β–dependent phosphorylation regulate its dynamic nuclear localization. C3G translocates to the nucleus in response to myogenic differentiation and sublethal dose of cisplatin. C3G is associated with chromatin and nuclear matrix fractions. Cells with C3G localized in the nucleus showed peripheralization of heterochromatin and reduced histone modifications associated with euchromatin. Short hairpin RNA–mediated depletion of C3G in epithelial cells resulted in reduced expression of CDK inhibitors and the histone demethylase KDM5A. Myoblast clones with CRISPR/Cas9-mediated knockout of C3G failed to show repression of histone marks and did not show up-regulation of myosin heavy chain and myotube formation when grown in differentiation medium. Our results document regulated nucleocytoplasmic exchange of C3G in response to physiological stimuli and provide insights into nuclear functions for C3G.**

Monitoring Editor
A. Gregory Matera
University of North Carolina

Received: Sep 14, 2016
Revised: Jan 24, 2017
Accepted: Jan 24, 2017

INTRODUCTION

The ubiquitously expressed guanine nucleotide exchange factor C3G (Rap guanine nucleotide exchange factor 1 [RapGEF1]) functions in signaling pathways to transmit information received by a variety of receptors and regulate cellular functions (Radha *et al.*, 2011). It is a 140-kDa protein with a C-terminal catalytic domain having GEF activity toward Ras family GTPases Rap1, Rap2, and R-Ras and Rho family GTPase TC10 (Gotoh *et al.*, 1995, 1997; Mochizuki *et al.*, 2000; Ohba *et al.*, 2001). About 300 residues in the central part of the molecule (Crk-binding region [CBR]) harbor a series of proline-rich sequences that are responsible for interaction with SH3 domain–containing molecules like Crk, HCK, and c-Abl, as well as non–SH3-containing proteins TC48 and β-catenin (Knudsen *et al.*, 1994; Shivakrupa *et al.*, 2003; Radha *et al.*, 2007; Mitra *et al.*, 2011; Dayma *et al.*, 2012). A deletion construct lacking N-terminal 579 amino acids is constitutively active, suggesting an inhibitory role for the noncatalytic region (Ichiba *et al.*, 1997). In addition to its catalytic functions, C3G can also engage signaling pathways through protein–protein interactions.

C3G primarily localizes to the cytoplasm and is engaged in regulating cell adhesion, actin remodeling, proliferation, suppression of transformation, and apoptosis (Radha *et al.*, 2011). It is essential for mammalian development, as knockout mice die before 7.5 d postcoitum (Ohba *et al.*, 2001). Altered expression of C3G (both high and low) is associated with human cancers (Hirata *et al.*, 2004;

This article was published online ahead of print in MBoC in Press (http://www.molbiolcell.org/cgi/doi/10.1091/mbc.E16-09-0660) on February 1, 2017.

*Address correspondence to: Vegesna Radha (vradha@ccmb.res.in).

Abbreviations used: CBR, Crk-binding region; CRM1, chromosome region maintenance 1; EHNA, erythro-9-[3-(2-hydroxynonyl)]adenine; GSK-3β, glycogen synthase kinase 3β; H3-Ac, H3 acetylation; H3K4me3, H4K4 trimethylation; HDAC, histone deacetylase; HP1, heterochromatin protein 1; LMB, leptomycin B; MHC, myosin heavy chain; NaB, sodium butyrate; N/C, nuclear to cytoplasmic; NES, nuclear export sequence; NLS, nuclear localization signal; N/W, nuclear to whole cell; RapGEF1, Rap guanine nucleotide exchange factor; TSA, trichostatin A.

© 2017 Shakyawar *et al.* This article is distributed by The American Society for Cell Biology under license from the author(s). Two months after publication it is available to the public under an Attribution–Noncommercial–Share Alike 3.0 Unported Creative Commons License (http://creativecommons.org/licenses/by-nc-sa/3.0).
"ASCB®," "The American Society for Cell Biology®," and "Molecular Biology of the Cell®" are registered trademarks of The American Society for Cell Biology.

Okino *et al.*, 2006; Fernandez *et al.*, 2008). In a context-dependent manner, it functions as an oncogene or anti-oncogene, suggesting that maintaining appropriate C3G levels and activity is important for tissue homeostasis. Phosphorylation at Y504 regulates C3G activity and is required for c-Abl–mediated apoptosis. Phosphorylated C3G localizes primarily to the Golgi and subcortical cytoskeleton and associates more strongly with cytoskeletal structures (Ichiba *et al.*, 1999; Radha *et al.*, 2004; Mitra and Radha 2010; Dayma and Radha, 2011). C3G is required for differentiation of neuronal cells and myocytes, and endogenous C3G is present in nuclei of differentiated myotubes (Radha *et al.*, 2008; Kumar *et al.*, 2015).

The function of proteins in a cell is often regulated by their localization to specific cellular compartments (Hung and Link, 2011). Dynamic exchange of signaling proteins between cytoplasmic and nuclear compartments in response to stimuli often determines gene expression and cellular outcomes such as proliferation, cell death, and differentiation (Gama-Carvalho and Carmo-Fonseca, 2001; Xu and Massague, 2004; Hall *et al.*, 2011). Generally, molecules larger than 50 kDa cannot passively move across the nuclear membrane and require selective transport mechanisms that depend on importins and exportins (Marfori *et al.*, 2011). These molecules recognize distinct amino acids as functional nuclear localization signal (NLS) or nuclear export sequence (NES) in the molecules to be transported (Pemberton and Paschal, 2005). In addition, posttranslational modifications, particularly phosphorylation, also regulate nucleocytoplasmic exchange of proteins (Nardozzi *et al.*, 2010).

C3G interacts with β-catenin and negatively regulates its transcriptional activity (Dayma *et al.*, 2012). Nuclear levels of β-catenin were particularly reduced in C3G-expressing cells. C3G interacts with E-cadherin, and many cadherin-binding proteins localize to the nucleus (Gottardi *et al.*, 1996; Hogan *et al.*, 2004; McEwen *et al.*, 2012). In silico analysis shows the presence of NLSs and an NES in C3G. We therefore examined whether C3G localizes to the nucleus in a regulated manner. We identify functional NLSs and NES in C3G and show that C3G is associated with the nuclear compartment in a dynamic manner in response to physiological stimuli. Nuclear C3G alters chromatin modifications, suggesting novel functions for C3G.

RESULTS

C3G is localized in the nucleus and accumulates in response to leptomycin B treatment

In immunofluorescence experiments, overexpressed as well as endogenous C3G primarily localizes to the cytoplasm (Hogan *et al.*, 2004; Radha *et al.*, 2004). Examination of the localization of C3G by subcellular fractionation and Western blotting in a variety of human cell lines showed that C3G is present in the nucleus as well as cytoplasm (Figure 1A). Purity of fractions was confirmed by probing the blots for nuclear (lamin B1) and cytoplasmic (calnexin) proteins. Actin was used as loading control, and levels of C3G in the nuclear and cytoplasmic fractions were determined. Averages obtained from multiple experiments showed difference in the nuclear levels of C3G in various cell types, with neuroblastoma cells (IMR-32) having high levels. Nuclear localization of C3G was not restricted to human cells, as myoblast cells from mouse also showed significant levels of C3G in the nucleus (see later discussion of Figure 7A).

The primary sequence of C3G has residues with features of NLSs and a leucine-rich NES (Figure 1B) and shows good conservation across species (Supplemental Figure S1). To determine whether C3G shows dynamic nucleocytoplasmic exchange, we examined Cos-1 cells expressing C3G for its localization in the presence or absence of leptomycin B (LMB), an inhibitor of chromosome region maintenance 1 (CRM1; Kudo *et al.*, 1999), a protein that functions primarily to export a large number of proteins from the nucleus and depends on leucine-rich nuclear export signals. Overexpressed C3G was predominantly cytoplasmic, with a small fraction of cells showing some staining in the nucleus. Quantitation of fluorescence in the nucleus relative to that in the whole cell (N/W) showed that LMB treatment results in an increase in level of C3G in the nucleus (Figure 1C). We obtained similar results by cell fractionation (Figure 1D).

Functional NES is present in the C-terminal of C3G

To test whether residues in the C-terminal showing consensus with typical NES (amino acids 776–791) are functional, we used deletion constructs of C3G that lack the catalytic (ΔC) or N-terminal (ΔN) domain or have only the CBR domain (Figure 1C). Whereas the full-length and ΔC constructs showed cytoplasmic localization in a majority of cells, CBR was primarily nuclear, and ΔN was exclusively cytoplasmic. Expression levels of these constructs shown by Western blotting (Supplemental Figure S2A) did not alter localization of the various proteins. In response to LMB treatment, a significantly higher proportion of cells expressing C3G as well as ΔC show nuclear staining (Supplemental Figure S2B), suggesting that the NES is functional in regulating nuclear export. Quantitation of the fluorescence intensity of C3G in the nucleus showed significant increase in nuclear C3G level on LMB treatment (Figure 1, D and E). LMB did not enhance nuclear localization of ΔN-C3G, which is unable to enter the nucleus. CBR has two putative NLSs and no NES and showed nuclear localization in the presence or absence of LMB. The relative ratio of nuclear versus cytoplasmic levels (N/C) of endogenous C3G was 1.4 ± 0.2–fold higher upon LMB treatment when examined by cell fractionation and averaged from multiple experiments (Figure 1E).

The ability of amino acids 776–791 to function as NES was examined directly by introducing these residues into a Rev–green fluorescent protein (GFP) expression vector (Henderson and Eleftheriou, 2000) and monitoring nuclear exit in response to LMB (Figure 2A). Rev-GFP shows exclusive nuclear localization, which is not sensitive to LMB. Introduction of C3G-NES sequences enables the protein to move into the cytoplasm (Figure 2, B and C). Nuclear export of Rev-NES-GFP having the NES sequence of Rev, which is sensitive to LMB, was used as a positive control (Wolff *et al.*, 1997).

The ability of these sequences to function as NES in the context of C3G was confirmed by site-directed mutagenesis of two leucines, LL779/781AA, in C3G-GFP (Figure 2D). Mutant NES (mNES)–expressing cells showed higher levels of nuclear protein than did wild type (WT; Figure 2, E and F). Whereas the WT responded to LMB treatment, the NES mutant did not, indicating that the two mutated leucine residues were indeed responsible for CRM1-mediated nuclear export. The NES mutant also showed increased association with the nucleus compared with WT in cell fractionation experiments (Figure 2G).

Nuclear localization of C3G is regulated by phosphorylation

C3G is a regulator and interacting partner of β-catenin (Dayma *et al.*, 2012). Because β-catenin localization is regulated by glycogen synthase kinase 3β (GSK-3β)–mediated phosphorylation, we tested whether C3G responds to inhibition of GSK-3β, a condition that mimics Wnt signaling. Treatment with LiCl, an inhibitor of GSK-3β (Stambolic *et al.*, 1996), induced nuclear translocation of overexpressed C3G in MCF-7 cells, as detected by immunofluorescence (Figure 3A) and cell fractionation (Figure 3B). Treatment of MDA-MB-231 cells with LiCl also enhanced nuclear levels of endogenous C3G (Figure 3C) and showed an increase in the relative nuclear levels upon cell fractionation (Figure 3D). Nuclear translocation of C3G

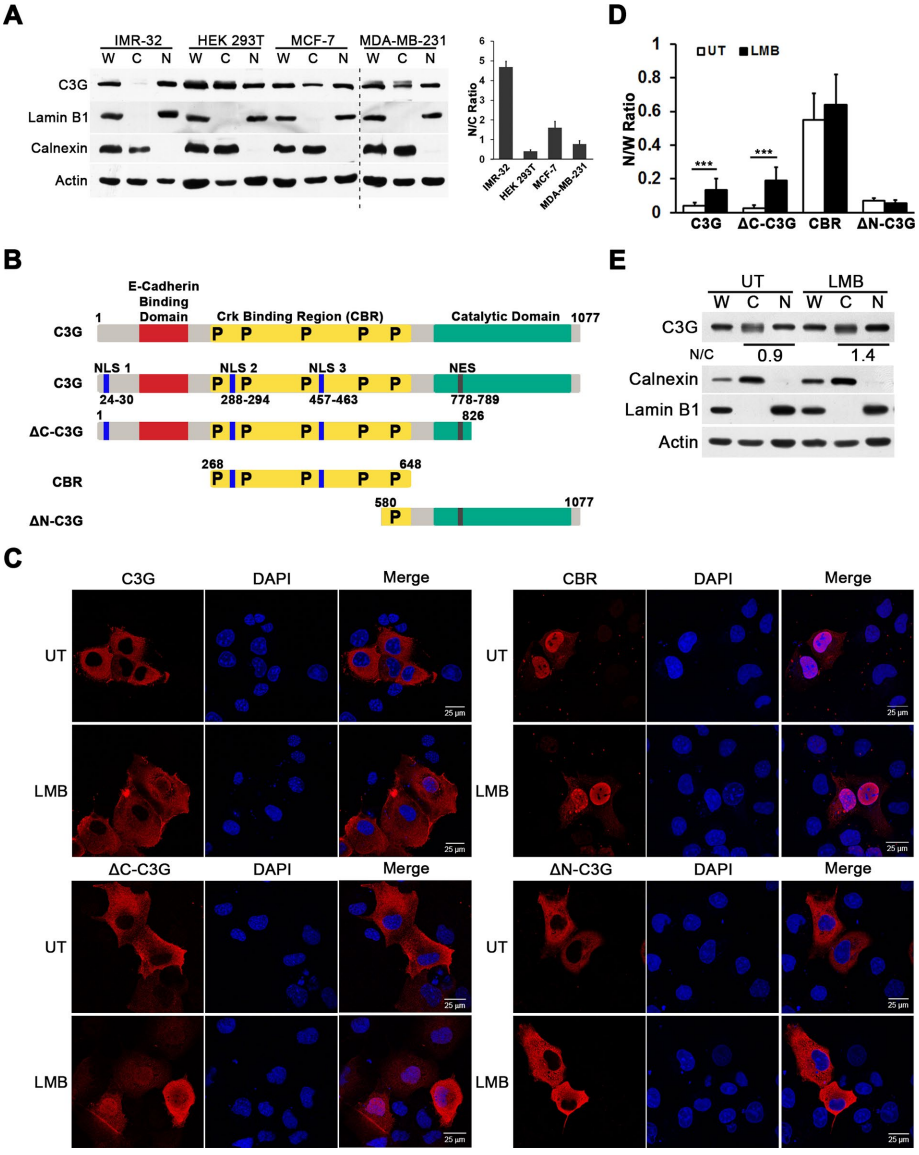

FIGURE 1: Nuclear localization of C3G. (A) Whole-cell lysates (W) and nuclear (N) and cytoplasmic (C) fractions were prepared from IMR-32, HEK 293T, MCF-7, and MDA-MB-231 cells and subjected to immunoblotting. Blot was probed for expression of C3G, lamin B1, calnexin, and actin. Lamin B1 and calnexin indicated purity of nuclear and cytosolic fractions, respectively. Actin was used as loading control. Lanes on the right of the vertical dashed line belong to a separate gel but were probed and exposed similarly. Right, bar diagram representing mean N/C ratio of C3G obtained by densitometric analysis from three independent experiments. (B) Schematic of C3G and its deletion constructs showing various domains, predicted NLSs, and NES (vertical lines). P indicates position of polyproline tracts. (C) Localization of exogenously expressed C3G and its deletion constructs in Cos-1 cells in the presence or absence of LMB. Images of a single *Z*-section through the center of the nucleus captured using a confocal microscope. (D) C3G and its deletion constructs were transiently expressed in Cos-1 cells in the presence or absence of LMB and subjected to immunostaining. Images captured were quantified for fluorescence intensity in the whole cell and its nucleus using ImageJ (Fiji) software. Bar diagram represents mean N/W ratio of fluorescence intensity from individual expressing cells belonging to three independent experiments. Horizontal lines indicate the sample sets compared for significance of difference. ***$p < 0.001$. (E) LMB treatment increases nuclear levels of C3G. Cell fractionation of MDA-MB-231 cells was carried out in the presence or absence of LMB, and fractions were analyzed by Western blotting using indicated antibodies. Numbers indicate N/C ratio of the levels of C3G in nuclear and cytoplasmic fractions, respectively.

was also examined by using an alternate inhibitor of GSK-3β, BIO, which increased nuclear levels of C3G and β-catenin (Supplemental Figure S3A).

In SDS–PAGE gels, endogenous C3G runs as a doublet of 140–145 kDa. A slow-moving band was seen in the cytoplasmic fraction of MDA-MB-231 cells but not in the nuclear fraction (Figures 1A and 3D). Because inhibition of GSK-3β caused nuclear translocation, we presumed that the mobility shift in C3G was caused by GSK-3β–mediated phosphorylation in the cytoplasm. We speculated that inhibition of GSK-3β will cause an increase in the N/C ratio of C3G, and inhibition of phosphatases may decrease it. This was verified by treating MDA-MB-231 cells with LiCl or okadaic acid (OA), an inhibitor of phosphatases PP1 and PP2A. Compared to untreated cells, the slow-moving band in the cytoplasmic fraction was significantly reduced by LiCl treatment and increased in OA-treated cells (Figure 3E), resulting in corresponding decrease or increase in N/C ratio. These results suggest that dynamic nucleocytoplasmic exchange of C3G is regulated by phosphorylation–dephosphorylation.

Nuclear translocation of many shuttling proteins is dependent on microtubules and dynein motors (Fazal *et al.*, 2007; Suárez-Sánchez *et al.*, 2014). Treatment with nocodazole significantly reduced levels of C3G-GFP in the nucleus of LiCl-treated cells, whereas cytochalasin D did not significantly alter the localization of C3G-GFP (Figure 3F and Supplemental Figure S3B). These inhibitors did not affect nuclear localization of C3G in the absence of LiCl treatment. Treatment with dynein inhibitor (erythro-9-[3-(2-hydroxynonyl)]adenine [EHNA]) also reduced LiCl-induced nuclear translocation of C3G (Figure 3G and Supplemental Figure S3C).

Nuclear translocation is dynamic and depends on functional NLS sequences

We examined whether nuclear translocation of C3G depended on a conventional importin-dependent pathway (Lange *et al.*, 2007). Coexpression of C3G with importin α4–GFP resulted in an increase in number of cells with nuclear C3G (Figure 4A), suggesting the presence of functional NLSs in C3G. We examined the response of various deletion constructs of C3G to LiCl treatment. The ΔN C3G, which lacks putative NLSs, primarily localized to the cytoplasm and did not translocate to the nucleus in response to LiCl (Figure 4B). Full-length and ΔC C3G showed nuclear translocation in response to LiCl, as shown by fluorescence intensity quantitation (Figure 4B) and cell fractionation (Supplemental Figure 2C).

Because CBR, which has two of the putative NLSs, showed constitutive nuclear localization, we created mutations that inactivated NLSs located within this region (Figure 5A). Each of the basic

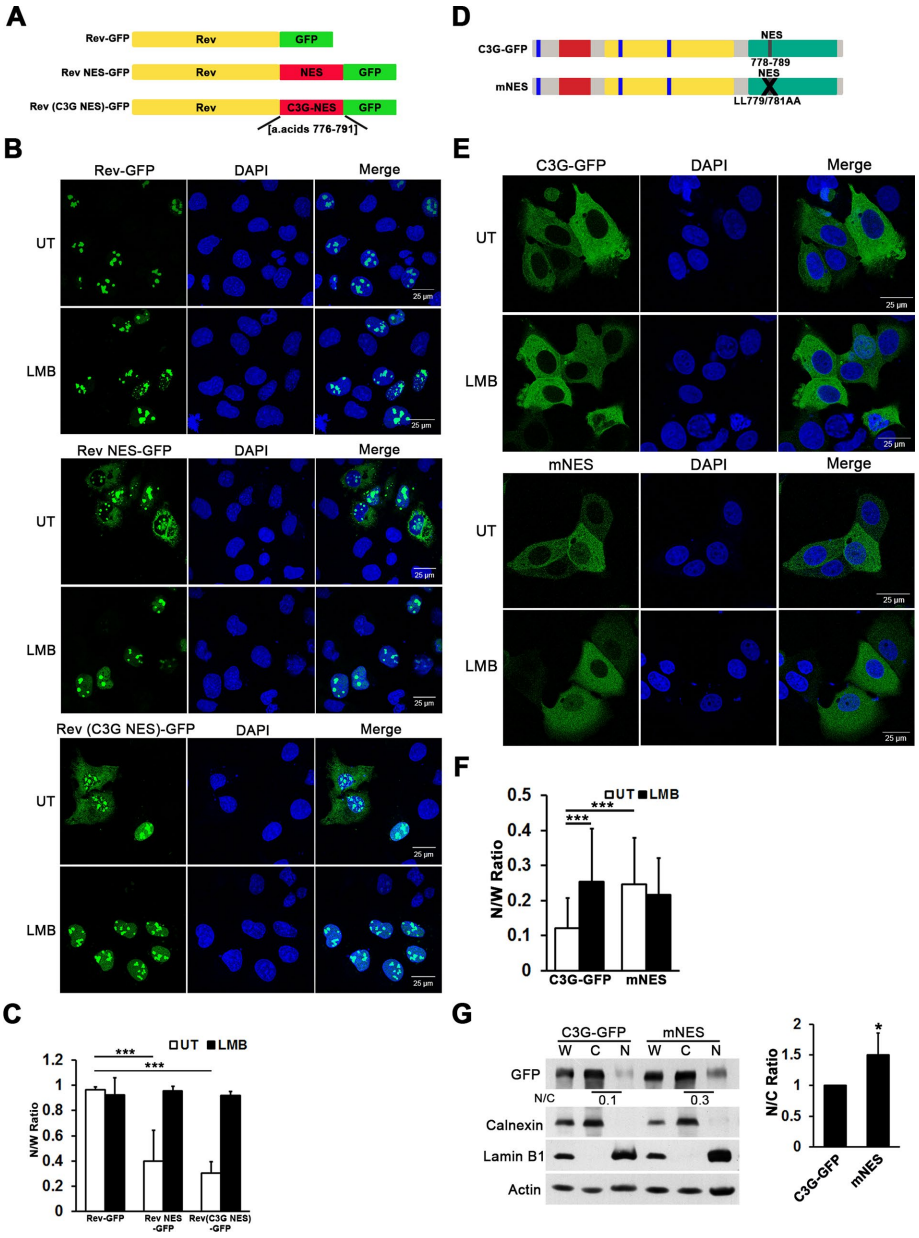

FIGURE 2: Identification of a functional NES in C3G. (A) Schematic of Rev-GFP, Rev NES-GFP, and Rev (C3G NES)-GFP fusion proteins. (B) Localization of the indicated Rev fusion proteins expressed in Cos-1 cells in the presence or absence of LMB. A single optical section captured using a confocal microscope. (C) Quantitation of the relative nuclear levels of the indicated proteins in cells from experiment in B plotted as mean ± SD from three independent experiments performed in duplicate. Horizontal lines indicate the sample sets compared for significance of difference. ***$p < 0.001$. (D) Schematic of C3G-GFP and NES mutant (mNES) indicating amino acid mutations made in the NES. (E) Localization of C3G-GFP and mNES expressed in MCF-7 cells in the presence or absence of LMB treatment. Single optical section captured using a confocal microscope. (F) Quantitation of the relative fluorescence intensity of C3G-GFP or mNES in the nucleus compared with that in the whole cell in the absence or presence of LMB. Data shown as mean ±SD from three experiments in duplicate. ***$p < 0.001$. (G) Cell fractionation of MCF-7 cells transfected with C3G-GFP and NES mutant was carried out and lysates subjected to Western blotting using indicated antibodies. Numbers indicate N/C ratio of the levels of C3G in nuclear and cytoplasmic fractions, respectively. Bar diagram shows mean N/C ratio from three independent experiments. *$p < 0.05$.

residues (lysine/arginine) at 290/291 and 460/461 in C3G-GFP was mutated to threonine (dm NLS) and examined for nuclear localization by immunofluorescence and cell fractionation. This mutant showed fewer cells with nuclear staining in the presence or absence of LiCl (Figure 5B). Significantly less of the mutant was associated with nuclear compartment compared with WT protein on LiCl treatment in cell fractionation experiments (Figure 5C).

We examined dynamic translocation of C3G into the nucleus by heterokaryon assay. C3G-GFP–transfected HeLa cells were fused with NIH3T3 cells and the presence of C3G in nuclei of 3T3 cells examined. In response to LiCl treatment, C3G showed pronounced localization to the 3T3 nucleus in hybrid cells (detected by pattern of 4′,6-diamidino-2-phenylindole [DAPI]; arrow in Figure 5D). GFP was used as control and showed passive movement into the 3T3 nucleus irrespective of LiCl treatment.

C3G is associated with chromatin fraction in the nucleus

Physiological stimuli regulate chromatin association of nuclear proteins to alter chromatin dynamics and gene expression (Badeaux and Shi, 2013). In the nucleus, overexpressed C3G was present in domains excluded from heterochromatin, indicated by counterstaining with DAPI and H3K9me3, a histone modification associated with inactive chromatin (Peters *et al.*, 2002; Supplemental Figure S4A). A change was also seen in organization of nuclear chromatin with heterochromatin prominently present at the nuclear periphery compared with nontransfected cells or transfected cells with C3G in the cytoplasm. (Figure 6A and Supplemental Figure S4A). Examination of C3G in various nuclear compartments of MDA-MB-231 cells showed its association with chromatin and nuclear matrix (Figure 6B). Soluble nuclear proteins leach into postnuclear supernatant when nuclei are prepared by detergent lysis, and some of the unbound nucleoplasmic C3G may be lost from the nuclear fraction. Fractionation of nuclei showed that endogenous C3G associated more with chromatin fraction in LiCl-treated MDA-MB-231 cells, suggesting that nuclear C3G can bind to and alter chromatin organization (Figure 6B). The blots were also probed for β-catenin, which shows enhanced association with chromatin in response to LiCl treatment (Jamieson *et al.*, 2011).

Change in chromatin dynamics is a consequence of histone modifications. H3K4 trimethylation (H3K4me3) and H3K9/K14 acetylation (H3-Ac) are marks associated with active genes or euchromatin (Wang *et al.*, 2008). These modifications were examined by immunofluorescence, and fluorescence intensity in the nucleus was quantitated. C3G-expressing cells treated with LiCl showed global reduction in

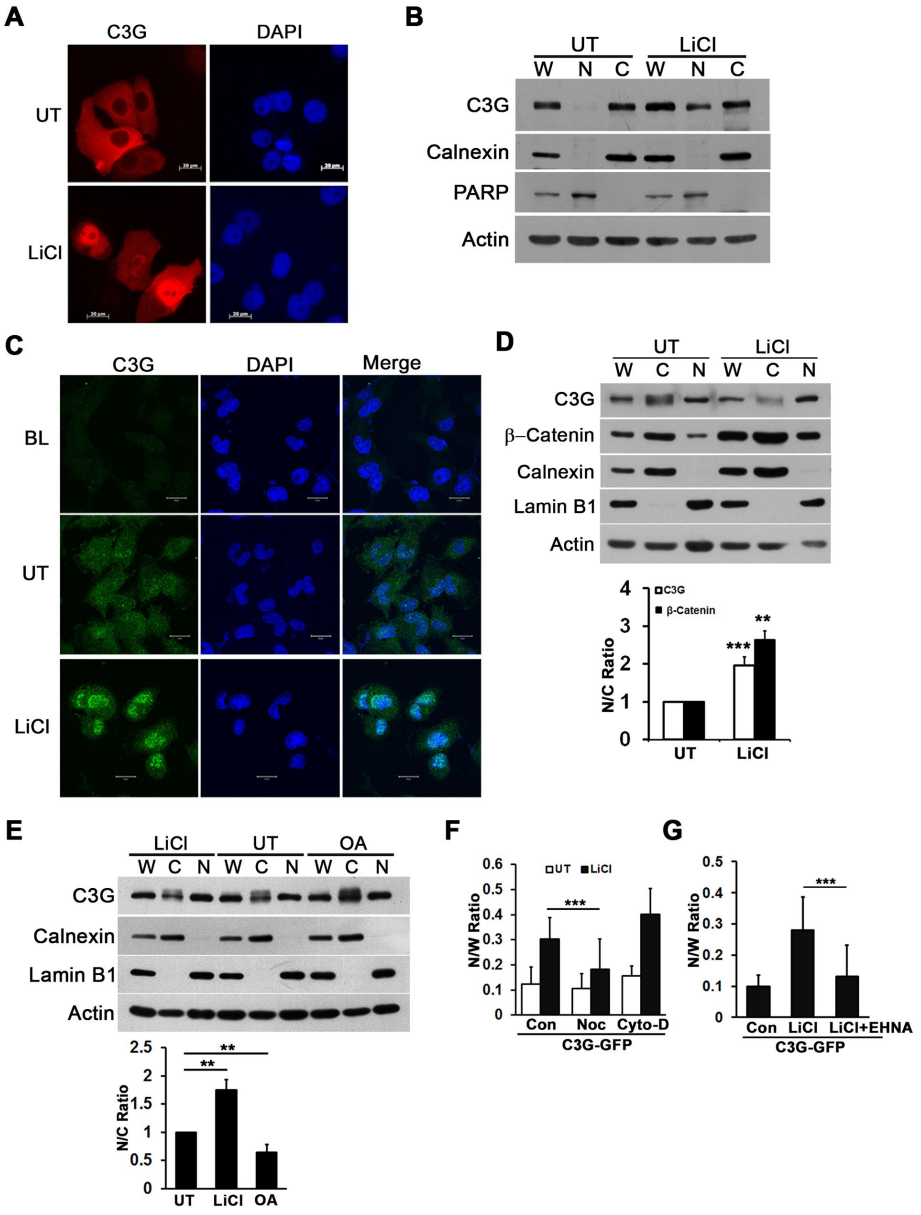

FIGURE 3: Inhibition of GSK-3β promotes nuclear entry of C3G. (A) MCF-7 cells transfected with C3G expression vector were either left untreated (UT) or treated with LiCl for 24 h, fixed with formaldehyde, and immunostained to detect C3G expression. Images captured using the 40× objective of a fluorescence microscope. (B) MCF-7 cells transfected with C3G expression vector were treated as in A and subjected to cell fractionation followed by Western blotting to detect indicated proteins. PARP was used as a marker for the purity of the nuclear fraction. (C) MDA-MB-231 cells plated on coverslips were left untreated or treated with LiCl, fixed with methanol, and stained for endogenous C3G. BL (blank), cells processed similarly but treated only with secondary antibody. (D) Cell fractionation of untreated and LiCl-treated MDA-MB-231 cells was performed followed by Western blotting to detect endogenous C3G and indicated proteins. Bar diagram represents the relative N/C ratio of C3G and β-catenin in response to LiCl treatment. Results are summarized from densitometric quantification of three experiments. $^{**}p < 0.01$; $^{***}p < 0.001$. (E) MDA-MB-231 cells were either left untreated or treated with LiCl or OA and cell fractionation performed. Fractions were subjected to Western blotting to detect indicated proteins, and relative changes in the nuclear-to-cytoplasmic levels of C3G are shown as average from three independent experiments. Horizontal lines indicate the sample sets compared for significance of difference. $^{**}p < 0.01$. (F, G) LiCl-induced nuclear translocation of C3G is dependent on microtubules and motor proteins. Cos-1 cells were transfected with C3G-GFP, left untreated, or treated with microfilament (Cyto-D), microtubule (nocodazole [Noc]), or dynein inhibitors (EHNA) as indicated. Fluorescence intensity in the nucleus relative to that in the whole cell was scored. Data represent averages taken from at least 25 cells from three independent experiments. $^{***}p < 0.001$.

both methylation and acetylation marks compared with untransfected cells or untreated cells with C3G in the cytoplasm (Figure 6, C and D, and Supplemental Figure S4B). The ability of C3G to repress H3 acetylation appears to be dependent on its N- and/or C-terminal sequences because CBR, which shows constitutive nuclear localization, did not alter H3-Ac marks (Supplemental Figure S4B). NES mutant of C3G, which is retained in the nucleus, caused a significant reduction in H3 acetylation even in the absence of LiCl treatment (Supplemental Figure S4C). These results suggest that nuclear C3G causes repression of marks associated with active chromatin. Histone deacetylase (HDAC) inhibition protects against deacetylation and demethylation of histones (Duque-Afonso *et al.*, 2011). The reduction of H3K4me3 (unpublished data), as well as H3 acetylation, caused by C3G was not observed in the presence of HDAC inhibitors trichostatin A (TSA) and sodium butyrate (NaB; Figure 6D), suggesting that C3G may be altering H3 acetylation by modulating HDAC activity. KDM5A is a primary enzyme responsible for demethylation of H3K4me3 (Christensen *et al.*, 2007; Klose *et al.*, 2007). We observed that cells with C3G knockdown by adenoviral short hairpin RNA (shRNA) construct showed significantly lower levels of KDM5A, suggesting that C3G modulates KDM5A levels to repress H3K4me3 (Figure 6E). The ability of C3G to undergo nucleocytoplasmic exchange and alter chromatin was suggestive of its ability to regulate gene expression. We showed previously that C3G overexpression induces p21 and p27 (Radha *et al.*, 2008; Kumar *et al.*, 2015). Knockdown of C3G using adenoviral vector expressing shRNA that targets C3G resulted in reduced expression of cell cycle inhibitors. These cells show enhanced levels of H3K4me3, indicating that C3G is required for maintaining levels of histone modifications and cell cycle inhibitors (Figure 6E).

C3G represses euchromatic histone modifications upon myocyte differentiation

We recently observed that C3G plays a role in differentiation of myocytes and localizes predominantly to the myotube nuclei, unlike in myoblasts, where it is primarily cytoplasmic (Kumar *et al.*, 2015). Subcellular fractionation showed relative enhancement in C3G associated with nuclear compartment in myotubes (Figure 7A). Differentiated human neuroblastoma cells, IMR-32, also showed an increase in nuclear levels of C3G (unpublished data), suggesting that nuclear

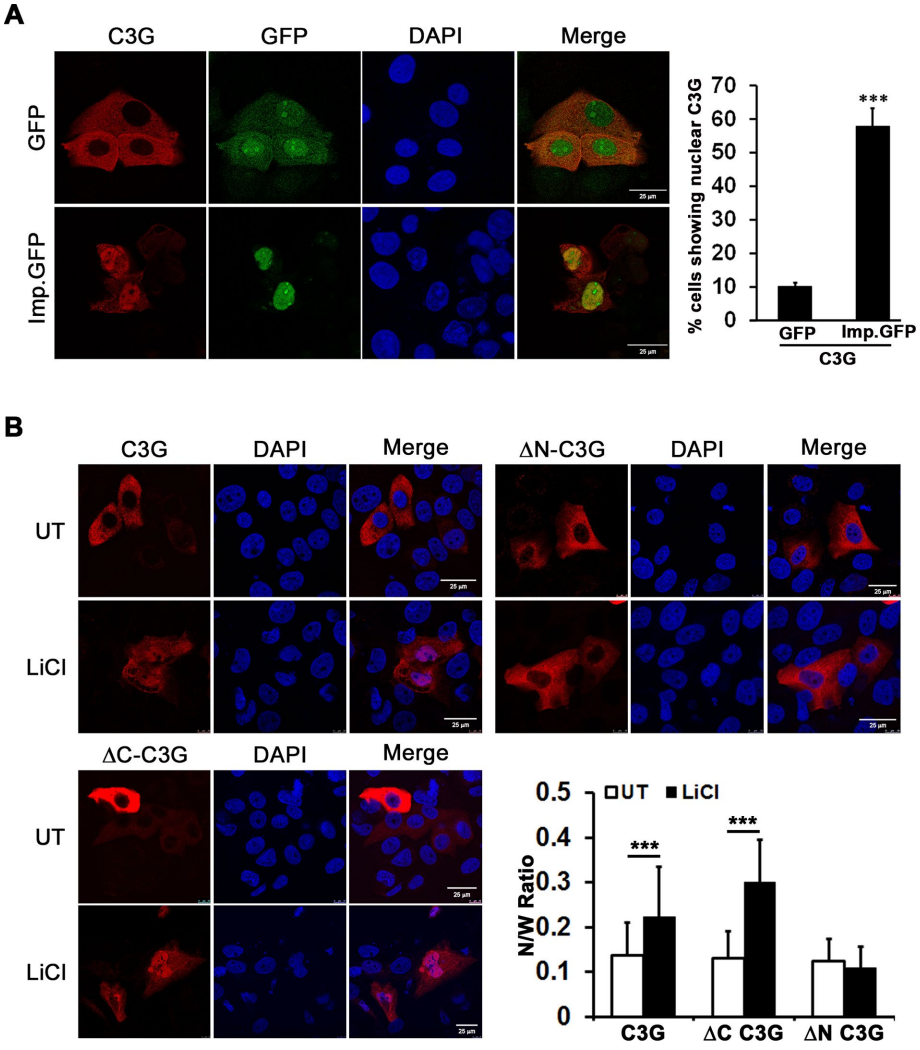

FIGURE 4: C3G has functional NLSs and undergoes importin-mediated nuclear translocation. (A) Cotransfection of C3G along with importin-α–GFP or GFP expression vectors was carried out in MCF-7 cells and C3G expression and localization detected by immunofluorescence. Single optical section through cells imaged from a confocal microscope. Bar diagram indicates percentage of cells showing nuclear localization of C3G in cells coexpressing C3G and GFP. ***$p < 0.001$. (B) MCF-7 cells transfected with C3G and its deletion constructs were grown in the presence or absence of LiCl. Cells were fixed with formaldehyde and immunostained for C3G. Images captured using a fluorescence microscope. Bar diagram shows relative nuclear levels of the indicated proteins compared with that in whole cell. Average of fluorescence intensity quantitation of ≥25 cells from three experiments. Horizontal lines indicate the sample sets compared for significance of difference. ***$p < 0.001$.

translocation of C3G is not restricted to differentiation of a single cell type.

To examine the effect of C3G translocation to myotube nuclei on chromatin reorganization, we generated stable clones of C2C12 lacking C3G via its knockdown using clustered regularly interspaced short palindromic repeats (CRISPR)/Cas technology. Knockout (KO) cells with little C3G expression did not show induction of myosin heavy chain (MHC) or formation of myotubes upon growth in differentiation medium (DM; Figure 7B). Immunofluorescence experiments showed that in control cells, C3G was present in myotube nuclei, which also showed peripheralization of heterochromatin unlike cells in growth medium (GM; Figure 7C). C3G was not present in nuclei of cells that did not fuse to form tubes. C3G-KO cells show no detectable C3G, and the heterochromatin pattern in KO cells was similar when cells were cultured in either GM or DM (Figure 7C). Control cells showed reduced H3-Ac in myotubes compared with cells grown in GM (Figure 7D). C3G-KO cells did not show reduction in H3-Ac when grown in DM. Mean signal intensity of H3-Ac and H3K4me3 is shown in Figure 7E. Lysates of C3G-KO cells showed enhanced levels of H3-Ac and H3K4 trimethylation (Figure 7F), suggesting that cellular C3G is required for maintaining levels of histone modifications. KO cells also showed reduced KDM5A expression, implying that reduction in levels of H3K4me3 by C3G may be achieved by altering KDM5A expression (unpublished data).

We also examined whether C3G showed nuclear translocation in response to other stimuli known to cause cell cycle arrest. Cisplatin treatment induces CDK inhibitors to arrest cell proliferation (Otto *et al.*, 1996; Zhu *et al.*, 2001). In response to sublethal dose of cisplatin, we observed translocation of endogenous C3G into the nucleus and an enhancement in ratio of nuclear levels to that in the whole cell (Figure 8, A–C). Efficacy of cisplatin treatment was confirmed by an increase in nuclear p53 levels. Enhanced association of C3G with chromatin fraction (1.6 ± 0.3–fold average change) was also seen (Figure 8D). Overexpressed C3G translocated to the nucleus, altered heterochromatin organization, and reduced H3-Ac upon cisplatin treatment (Figure 8F). Reduced levels of H3K4me3 were also observed in cisplatin-treated cells, in which endogenous C3G translocates to the nucleus (unpublished data).

DISCUSSION

Studies on subcellular localization of a protein and its dynamic translocation to distinct compartments in response to physiological stimuli helps in understanding its cellular functions. This study unequivocally shows that C3G (RapGEF1), a large protein of ~140 kDa can localize to the nucleus and regulate processes in this compartment. Although overexpressed C3G was previously shown to primarily localize to the cytoplasm (Guerrero *et al.*, 1998; Hirata *et al.*, 2004; Hogan *et al.*, 2004; Radha *et al.*, 2004), we find that the endogenous protein, in a battery of human cell lines, is associated with nuclei when cells are fractionated. It was also found that the amount of C3G associated with nuclear compartment in exponentially growing cells differs in various cell lines, suggesting that it may serve specific nuclear functions, depending on cell type.

As anticipated, we found functional NES and NLSs in C3G and that its nuclear import and export are regulated by importin and CRM1, respectively. The functional NLSs are present in central domain–containing, proline-rich sequences, primarily shown to be responsible for interaction with a variety of proteins (Radha *et al.*, 2011). Mutation of both sites in the CBR domain did not totally

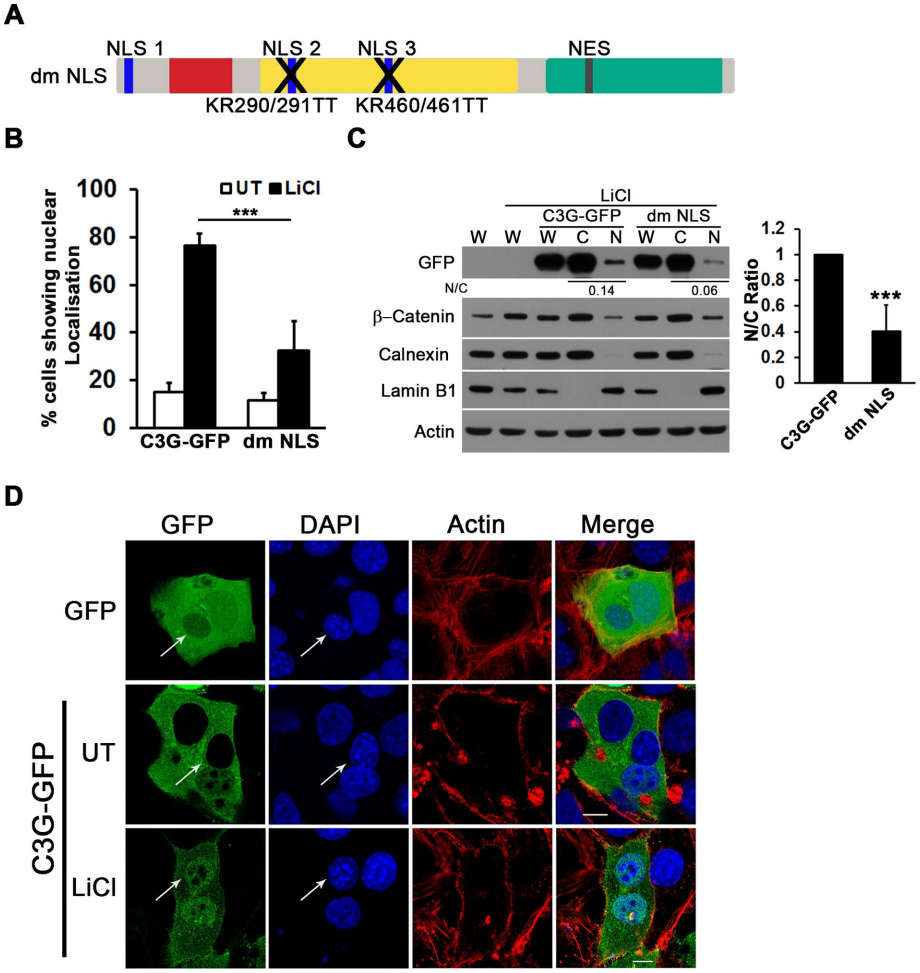

FIGURE 5: Dynamic nuclear translocation of C3G is dependent on NLSs. (A) Schematic of dm NLS indicating mutations in residues corresponding to NLS 2 and 3. (B) MCF-7 cells expressing C3G-GFP or dm NLS either untreated or treated with LiCl were subjected to immunofluorescence and proportion of cells with nuclear GFP quantitated. Data obtained from three independent experiments in duplicate. Horizontal line indicates the sample sets compared for significance of difference. ***$p < 0.001$. (C) Untransfected MCF-7 or cells expressing C3G-GFP or dm NLS were treated with LiCl and subject to cell fractionation followed by Western blotting with indicated antibodies. Bar diagram shows relative difference in N/C ratio of dm NLS compared with C3G-GFP averaged from three experiments. ***$p < 0.001$. (D) HeLa cells were transfected with either C3G-GFP or GFP expression vectors. The transfected cells were subjected to an interspecies heterokaryon assay using NIH3T3 cells. After fixation, fused cells were detected by staining for actin using rhodamine–phalloidin and DAPI to detect nuclei. Cells were examined for hybrid cells with GFP expression. A single optical section through the center of nuclei captured using a confocal microscope. Arrows indicate nuclei of NIH3T3 cells fused with HeLa cells.

compromise nuclear translocation, and it is possible that the sequence in the N-terminal region also contributes to nuclear localization in full-length C3G. A functional NES was identified at the C-terminal residues 778–789, which enabled CRM1-dependent export. It was observed that endogenous C3G was more responsive to LMB or LiCl treatment than with overexpressed C3G. A deletion mutant having the NES at the extreme C-terminal and lacking the catalytic domain is more responsive to LMB treatment than the full-length C3G, suggesting that in the cellular context, the catalytic domain may partly mask the NES. Comparison of the primary C3G sequence across species showed that the two functional NLSs and the NES are conserved, indicating that C3G may have nuclear functions in other organisms as well.

We also provide evidence for dynamic and regulated nucleocytoplasmic exchange of C3G. Enhanced nuclear localization is triggered upon inhibition of GSK-3β, suggesting that nuclear translocation may be regulated by phosphorylation. Indeed, a slow-moving band is seen only in cytoplasmic fraction, and inhibition of dephosphorylation by okadaic acid results in an increase in the levels of slow-moving C3G. Both PP1 and PP2A are inhibited by okadaic acid; therefore, we could conclude that C3G is a substrate of one or both these enzymes. A significant amount of active PP1 is present in the nuclear compartment and associated with chromatin (Kuret *et al.*, 1986). It is likely that this arrangement keeps nuclear C3G in a dephosphorylated state and regulates its exit. C3G interacts with PP2A (Martín-Encabo *et al.*, 2007), and it is therefore possible that GSK-3β and PP1/PP2A activities regulate its dynamic movement between the nucleus and cytoplasm in a stimulus-dependent manner.

An heterokaryon assay demonstrated that accumulation of C3G in the nucleus is an active process compared with movement of GFP, a small molecule that can passively move through nuclear pore. Cytoskeleton is known to aid nuclear import of proteins (Moseley *et al.*, 2007; Roth *et al.*, 2007). Nuclear translocation of C3G was dependent on microtubule- and dynein-dependent transport. C3G was previously shown to bind to actin (Martín-Encabo *et al.*, 2007) and cytoskeletal elements (Dayma and Radha, 2011), and this feature may be responsible for its translocation. In addition to conditions mimicking Wnt signaling by pharmacologically blocking GSK-3β activity, C3G translocated to the nucleus in response to a sublethal dose of cisplatin—DNA-damaging agent—and also in response to differentiation of myocytes and neuronal cells. C3G has multiple predicted sites for phosphorylation by a variety of kinases in addition to GSK-3β. Translocation of C3G into the nucleus during cisplatin treatment or myocyte differentiation may also be dependent on phosphorylation. Differentiation signals could inhibit GSK-3β activity (Knight and Kothary, 2011), causing nuclear translocation of C3G. CDK5 activity increases during myogenic and neuronal differentiation, and C3G is a substrate of CDK5 (Utreras *et al.*, 2013). It remains to be determined whether CDK5-mediated phosphorylation promotes nuclear translocation of C3G.

We see that nuclear C3G is associated with both chromatin and nuclear matrix, and its association with chromatin increases upon LiCl as well as cisplatin treatment. Cells with nuclear C3G showed repression of histone modifications associated with active chromatin, indicating that C3G can cause global changes in gene expression. Change in global histone methylation pattern is associated with pluripotency (Mattout *et al.*, 2011) and oncogenicity

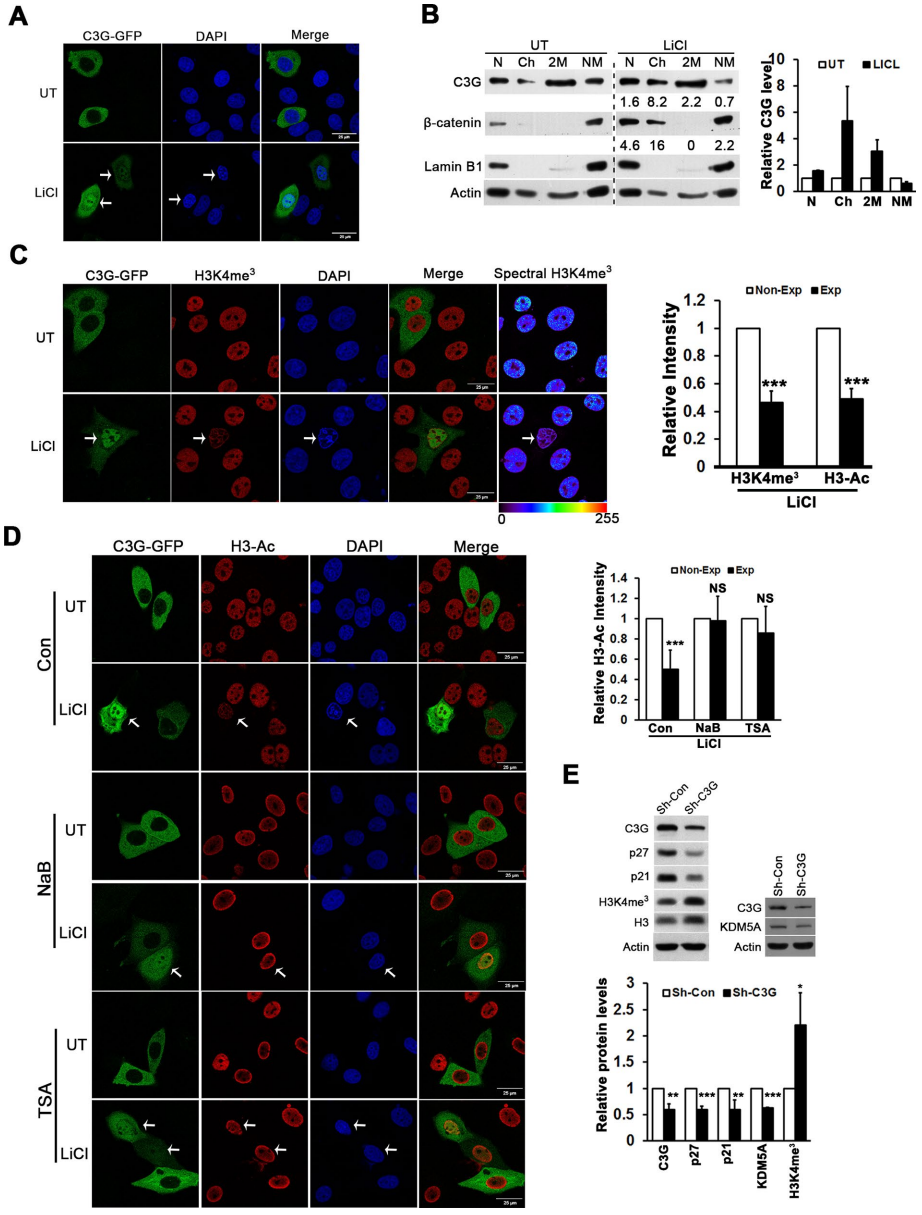

FIGURE 6: C3G associates with chromatin and represses euchromatic histone marks. (A) MCF-7 cells transfected with C3G-GFP were left untreated or treated with LiCl before fixation. Arrows indicate cells with nuclear C3G and peripheralization of the heterochromatin. (B) Untreated or LiCl-treated MDA-MB-231 cell nuclei (N) were further fractionated into chromatin (Ch), high-salt extract of chromatin (2M), and nuclear matrix (NM) followed by Western blotting for the indicated proteins. Lamin B1 was used as a marker for nuclear matrix, and β-catenin was used as positive control for LiCl treatment. Bar diagram indicates relative change in C3G in different nuclear fractions of LiCl-treated cells compared with untreated cells averaged from three experiments. (C) MCF-7 cells transfected with C3G-GFP were left untreated or treated with LiCl followed by immunofluorescence to detect H3K4me3. A single section through the nuclei of cells analyzed on a confocal microscope. H3K4me3 intensity is also shown in spectral color to better depict fluorescence intensity difference in cells with nuclear C3G. Bar at bottom represents range of signal intensity from violet (low) to red (high). Signal intensities were quantified using LAS software. Graph shows relative signal intensities of H3K4me3 and H3-Ac modifications in the nuclei of LiCl-treated, C3G-expressing cells compared with nonexpressing cells. ***$p < 0.001$. (D) Effect of C3G on histone modification depends on histone deacetylases. MCF-7 cells expressing C3G-GFP and grown in the presence or absence of LiCl were in addition treated with NaB or TSA. Cells were fixed and immunostained with H3-Ac. Bar diagram shows relative H3-Ac intensity from expressing and nonexpressing cells with indicated treatments. ***$p < 0.001$. (E) C3G knockdown alters histone modifications and expression of various proteins. MCF-7 cells were infected with Sh-C3G or control adenoviral particles and grown for 90 h. Lysates were subjected to immunoblotting, and blot was probed for indicated proteins. Bar diagram shows relative levels of the proteins averaged from three independent experiments. *$p < 0.05$; **$p < 0.01$; ***$p < 0.001$.

(Martinez-Garcia *et al.*, 2011). The effect of C3G is mediated through histone deacetylases, as their inhibition compromises the ability of C3G to suppress both H3-Ac and H3K4me3. These modifications on histones are coupled, as HDAC inhibitors alter acetylation as well as methylation (Duque-Afonso *et al.*, 2011). It is also likely that C3G modulates histone trimethylation by regulating levels of KDM5A, as cells with C3G knockdown showed reduced KDM5A levels and increased H3K4me3. Protein transport into the nucleus and changes in chromatin organization occur during muscle cell differentiation (Moen *et al.*, 2004; Hall *et al.*, 2011), and myocyte differentiation is modulated by H3K4me3 (Milne *et al.*, 2005). H3K4me3 is low after 2 d of C2C12 differentiation (Londhe and Davie, 2013), and C2C12 cells with C3G knocked down do not show this repression or express MHC.

β-Catenin signaling promotes H3K4me3 (Wend *et al.*, 2013). The effect of C3G on regulation of H3K4me3 agrees with its role as a negative regulator of β-catenin. Induction of growth arrest is a feature common to DNA damage and differentiation signals. It is therefore possible that C3G translocates to the nucleus to control expression and activity of transcription factors to regulate gene expression. Reduced expression of cell cycle inhibitors p27 and p21 in cells with C3G knockdown is suggestive of this function. Heterochromatin protein 1 (HP1) proteins enable establishment of proper chromatin structure, and improper heterochromatin arrangement is associated with diseases and developmental disorders (Hahn *et al.*, 2010). C3G has sequences in its C-terminal domain that could function as a chromo-shadow domain–binding sequence and therefore could interact with HP1. This is being investigated. Altered chromatin modification may be a mechanism by which C3G causes changes in cellular responses to physiological stimuli.

In conclusion, we show that dynamic exchange of C3G between nuclear and cytoplasmic compartments is regulated by 1) functional NLSs and NES in its primary sequence, 2) importin- and exportin-mediated transport, and 3) phosphorylation and

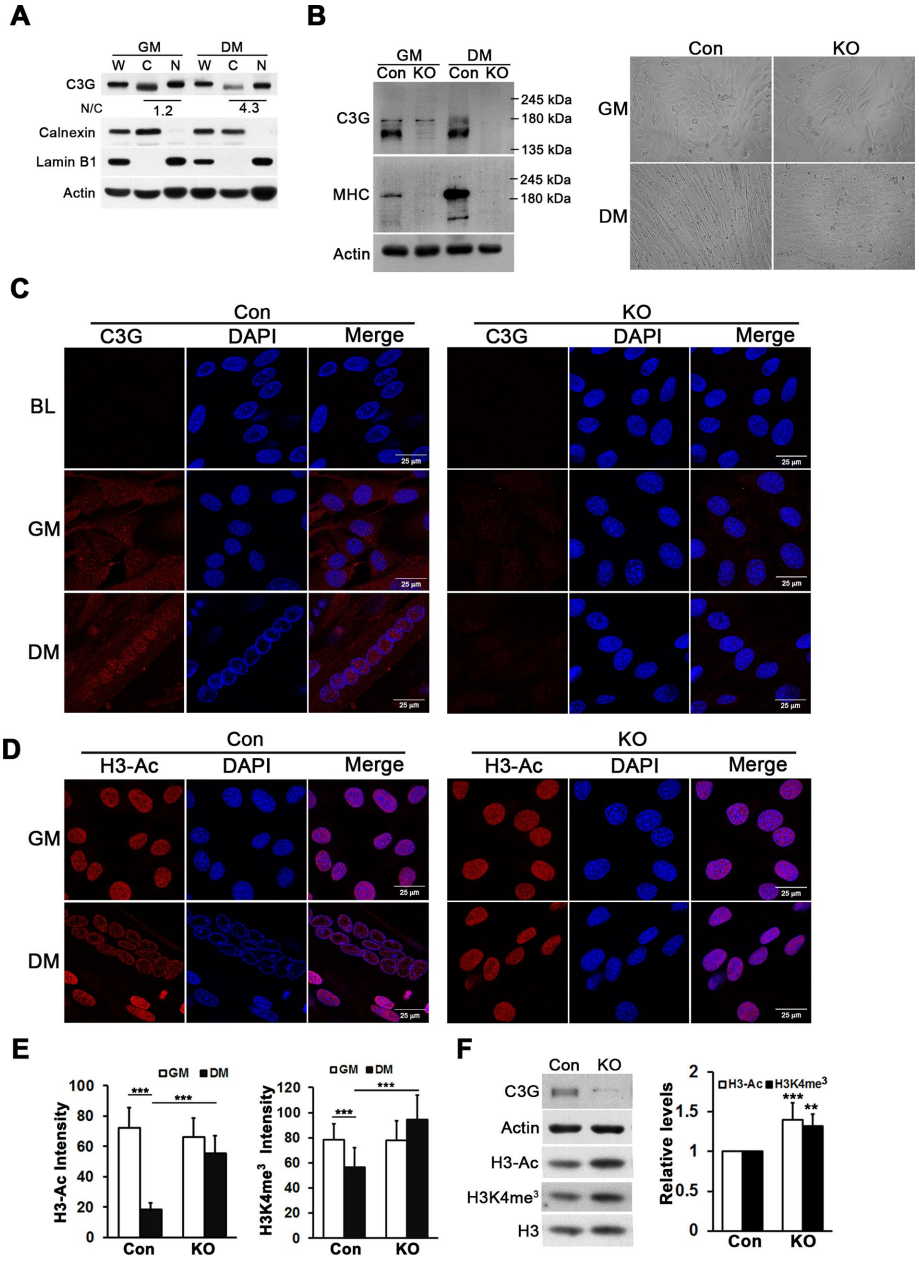

FIGURE 7: Nuclear translocation of C3G upon differentiation affects histone modifications in C2C12 myocytes. (A) C2C12 cells were grown in GM or DM for 96 h and subjected to cell fractionation and Western blotting for examining levels of C3G, calnexin, lamin B1, and actin. Numbers indicate N/C ratio of the levels of C3G in nuclear and postnuclear fractions. (B) C3G CRISPR knockout clone (KO) and control (Con) clone were grown in the presence of GM or DM for 72 h and lysates subjected to Western blotting. Blot was probed for expression of C3G, MHC, and actin. Images show morphology of control and C3G-knockout clone under conditions of culture in growth medium or differentiation medium. (C) Control and C3G KO clone were grown for 96 h, fixed, and immunostained for C3G. Single optical section taken through the center of nuclei using a confocal microscope. (D) Control and C3G KO clones were immunostained for H3-Ac. (E) Signal intensities of H3-Ac and H3K4me3 from control and C3G KO clone grown in GM or DM. Horizontal lines indicate sample sets compared for significance of difference. ***$p < 0.001$. (F) Lysates of control and C3G KO clones were subjected to Western blotting and probed for C3G, H3-Ac, H3K4me3, H3, and actin. Quantitation of H3-Ac and H3K4me3 adjusted to total H3 protein from three independent experiments. **$p < 0.01$; ***$p < 0.001$.

dephosphorylation mediated by GSK-3β and protein phosphatases. C3G translocates to the nucleus in response to treatments mimicking Wnt signal activation, myogenic differentiation, and DNA damage. C3G regulates KDM5A levels and HDAC activity, resulting in global changes in histone modifications associated with euchromatin. These results are presented as a model (Figure 8F). Altered gene expression and inability to differentiate in response to loss of C3G may be a consequence of C3G's role in regulating chromatin modifications.

MATERIALS AND METHODS

Expression constructs

Mammalian vector for expression of C3G (pcDNA3-Flag C3G) was gifted by S. Tanaka (The Rockefeller University, New York; Tanaka *et al.*, 1994). Truncated constructs of C3G, ΔN-C3G, ΔC-C3G, and CBR have been described (Ichiba *et al.*, 1999; Schmitt and Stork, 2002). C3G cloned into pEGFP-N3 has been described (Dayma and Radha, 2011). C3G with mutations in two NLS sites (dm NLS) was generated by sequential mutagenesis at KR460/461TT (NLS 3) and KR290/291TT (NLS 2) in C3G-GFP vector by substitution of Lys/Arg codons with threonine. Rev-GFP and Rev-NES-GFP were provided by Beric Henderson (Westmead Institute, Australia). Rev(C3G-NES)-GFP construct was generated by cloning C3G-NES (amino acids 776–791) into Rev-NES-GFP at *Bam*HI and *Age*I sites after excising out the default NES. Importin-α4 construct was a gift from Ghanshyam Swarup (Center for Cellular and Molecular Biology, Hyderabad). The mNES C3G-GFP construct was generated by mutagenesis in C3G-GFP (LL779/781AA) vector. shRNA adenoviral vector to knock down human C3G was generated using an AdEasy System provided by Bert Vogelstein (Howard Hughes Medical Institute). shRNA sequence targeting human C3G has been described (Radha *et al.*, 2007).

Cell culture, transfections, and treatments

Cos-1, MCF-7, IMR-32, HeLa, NIH3T3, HEK293T, and MDA-MB-231 were obtained from the American Type Culture Collection and cultured in DMEM containing 10% fetal calf serum (FCS) at 37°C in 5% CO_2 humidified chamber. Mouse myoblast cells, C2C12, were cultured in DMEM with 20% FCS. C2C12 and IMR-32 differentiation was carried out as described (Radha *et al.*, 2008; Kumar *et al.*, 2015). For transfections, Lipofectamine 2000 or Lipofectamine 3000 from Invitrogen was used. For transfecting Cos-1 cells, cationic lipid DHDEAB was used as described (Banerjee *et al.*, 1999). Treatments with LiCl (Sigma-Aldrich), 50 mM, 24 h; OA (Boehringer Mannheim), 20 nM, 20 h; LMB (Calbiochem), 37 nM, 6 h; EHNA (Sigma-Aldrich), 10 μM, 24 h; cisplatin (Sigma-Aldrich), 25 μM, 2 h;

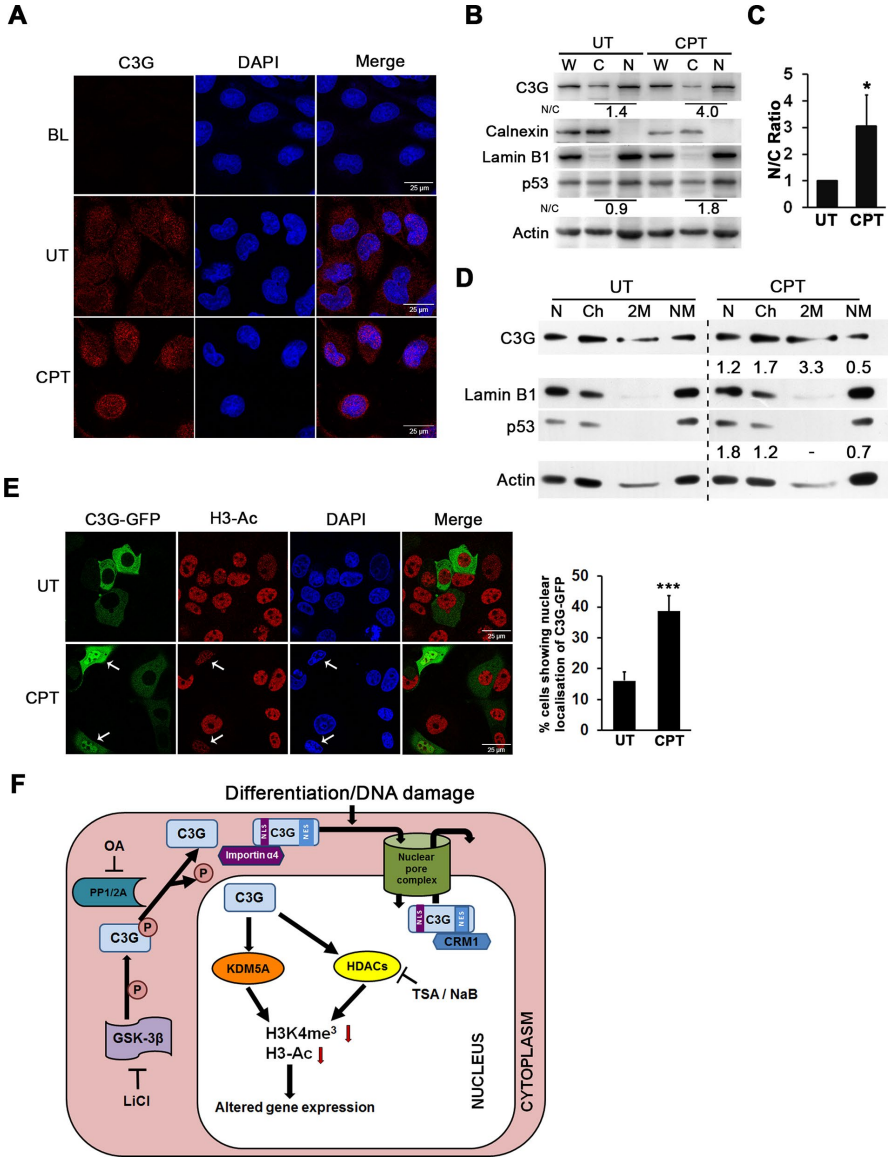

FIGURE 8: C3G translocates to the nucleus upon cisplatin (CPT) treatment. (A) MDA-MB-231 cells were grown in the presence or absence of CPT, fixed with methanol, and stained for endogenous C3G. A single section captured through the center of the nucleus using a confocal microscope. (B) Normally growing or CPT-treated MCF-7 cells were subject to cell fractionation followed by Western blotting to detect indicated proteins. p53 was used as control to indicate efficacy of CPT treatment. (C) Relative N/C ratio of C3G in MCF-7 cells obtained from densitometric quantification of Western blot bands from three independent experiments. *$p < 0.05$. (D) Untreated and CPT-treated cell nuclei (N) were further fractionated into chromatin (Ch), high-salt extract of chromatin (2M), and nuclear matrix (NM) followed by Western blotting for the indicated proteins. Lamin B1 was used as a marker for nuclear matrix. p53 was used as positive control for CPT treatment. Numbers indicate relative change in C3G and p53 in different nuclear fractions of CPT-treated cells compared with untreated cells. (E) MCF-7 cells transfected with C3G-GFP vector were given CPT treatment before formaldehyde fixation and immunostained for H3-Ac. Arrows show cells with C3G in nucleus and reduced H3-Ac. Bar diagram shows the percentage of cells with C3G-GFP in nucleus. ***$p < 0.001$. (F) Schematic model depicting regulation of nucleocytoplasmic exchange of C3G and its role in chromatin remodeling and gene expression. Phosphorylation (mediated by GSK-3β) retains C3G in the cytoplasm, and its dephosphorylation (mediated by PP1/2A) causes its translocation into the nucleus, depending on functional NLS in its primary sequence. An NES in its C-terminal enables CRM1-mediated export from the nucleus. Stimuli that cause cell cycle arrest (growth of myoblasts in differentiation medium or cisplatin treatment of epithelial cells) promote nuclear translocation of C3G to cause repression of histone modifications H3K4me3 and H3-Ac. Cells lacking C3G show decreased KDM5A histone demethylase, and HDAC inhibitors protect against C3G-induced repression of histone marks. Loss of C3G causes decrease in expression of cell cycle inhibitors p21 and p27.

TCA (Sigma-Aldrich), 600 nM, 12 h; NaB (Sigma-Aldrich), 10 mM, 12 h; cytochalasin D (Calbiochem), 0.2 µg/ml, 4 h; and nocodazole (Calbiochem), 1µg/ml, 4 h were done by incubating exponentially growing cells with respective drug(s) in cell culture medium. In case of transfections, treatment endpoints coincided with 30 h posttransfection.

For generating C3G KO stable clones, C2C12 cells were cotransfected with C3G CRISPR/Cas9 KO plasmid (sc-430750) and HDR plasmid (sc-430750-HDR). After 30 h of expression, cells were selected in puromycin. Early-passage cells that showed near-complete loss of C3G expression were used for all experiments.

Antibodies and reagents

Rabbit polyclonal C9 antibody used for detection of overexpressed C3G and its truncated constructs was generated in our lab (Radha *et al.*, 2007). C3G, calnexin, β-catenin, p27, p53, GFP, and MHC antibodies were from Santa Cruz Biotechnology. H3K4me3, H3-Ac, H3, p21, and actin antibodies were from Millipore. Lamin B1, KDM5A, and PARP antibodies were from Abcam and Roche. Cells were stained for F-actin using rhodamine–phalloidin (Molecular Probes).

Western blotting, immunofluorescence, and nuclear fractionation

Western blotting was performed as described (Radha *et al.*, 2004). Detection of bands was carried out using a Kodak XBT autoradiogram or Vilber-Lourmat Chemiluminescence System (Germany). The quantification of Western blots was carried out using ImageJ software, and values were normalized to the loading control. Immunostaining was performed as previously described (Shivakrupa *et al.*, 2003). Images were acquired using a Leica TCS SP8 microscope (Leica Microsystems, Germany) and an Axioimager Z1 fluorescence microscope from Carl Zeiss (Germany) and were analyzed using Image J (Fiji), Leica Application Suite, or AxioVision 4.4 software. Acquisition parameters were maintained constant for capture of images of all samples from a particular experiment. Quantitation of cells with distinct subcellular localization of desired proteins was performed using the 40× objective of an Olympus fluorescence microscope by analyzing >200 cells/coverslip. Averages were obtained from at least three independent experiments carried out on duplicate coverslips. Quantitation of the fluorescence intensity was carried out using ImageJ software after image acquisition using a confocal

microscope. Quantitation of the C3G in the nucleus was carried out from the images by analyzing fluorescence intensity in the nucleus and comparing it with that in the whole cell. Cells with similar levels of expression of the indicated proteins were chosen for quantitation. The average of relative levels in the nucleus was taken from >25 cells from each experimental condition and repeated thrice on duplicate coverslips. For quantitation of fluorescence signal intensity of histone marks (H3-Ac and H3K4me3), total signal intensity from 50-μm^2 regions of interest within the nucleus was collected from nonexpressing and C3G-expressing cells from the same coverslip. From 50 to 100 nuclei were analyzed in each experiment. Samples of cell lysates (W) and nuclear (N) and cytoplasmic (C) fractions were prepared as described (Radha *et al.*, 1994). Similar amounts of total protein were loaded, and relative level of a protein in nuclear versus cytoplasmic compartment (N/C) was assessed after normalizing with loading control. Preparation of chromatin (Ch) and nuclear matrix (NM) fractions has been described (Radha *et al.*, 1994).

In silico analysis of nuclear export and import sequences

In silico prediction of NLS in C3G was done using the PSORT II Prediction server (http://psort.hgc.jp/form2.html; Horton and Nakai, 1997), the NucPred tool (www.sbc.su.se/~maccallr/nucpred/cgi-bin/single.cgi; Brameier *et al.*, 2007), and NLStradamus tools (www.moseslab.csb.utoronto.ca/NLStradamus/; Brameier *et al.*, 2007; Ba *et al.*, 2009). Residues commonly identified by all three programs were considered as putative NLSs. Prediction of leucine-rich NES in C3G was done on NetNES 1.1 Server (www.cbs.dtu.dk/services/NetNES; La Cour *et al.*, 2004).

Heterokaryon assay

HeLa cells transfected with C3G-GFP for 36 h, were mixed with an equal number of NIHT3T3 cells (70,000 each) and plated on glass coverslips. After overnight attachment, cells were treated with cyclohexamide (100 μg/ml) for 30 min, washed with phosphate-buffered saline (PBS), and incubated for 2 min at 37°C in a solution containing poly(ethylene glycol) (Mr = 3300) and PBS in a 1:1 ratio (vol/vol). After being washed in PBS and in plain medium, cells were incubated in complete medium containing cyclohexamide for 4 h in the presence or absence of LiCl. Cells were fixed in formaldehyde, permeabilized, and stained with DAPI and phalloidin before mounting.

Statistical analysis

All data are reported as mean ± SD. Student's *t* test was used to determine the significance of differences in means.

ACKNOWLEDGMENTS

We thank S. Tanaka, M. Matsuda, P. J. S. Stork, Beric R. Henderson, Bert Vogelstein, and G. Swarup for gifts of valuable plasmids. D.K.S. acknowledges a fellowship from the Council of Scientific and Industrial Research, Government of India. This work was supported by funds from the Council of Scientific and Industrial Research, Government of India (BSC 0115, BSC 0108, and BSC 0111). Support was also received from the Department of Science and Technology (SR/SO/BB/087/2012) and the Department of Biotechnology, Government of India (BT/PR11759/BRB/10/1301/2014).

REFERENCES

Badeaux AI, Shi Y (2013). Emerging roles for chromatin as a signal integration and storage platform. Nat Rev Mol Cell Biol 14, 211–224.

Banerjee R, Das PK, Srilakshmi GV, Chaudhuri A, Rao NM (1999). Novel series of non-glycerol-based cationic transfection lipids for use in liposomal gene delivery. J Med Chem 42, 4292–4299.

Brameier M, Krings A, MacCallum RM (2007). NucPred—predicting nuclear localization of proteins. Bioinformatics 23, 1159–1160.

Christensen J, Agger K, Cloos PA, Pasini D, Rose S, Sennels L, Rappsilber J, Hansen KH, Salcini AE, Helin K (2007). RBP2 belongs to a family of demethylases, specific for tri-and dimethylated lysine 4 on histone 3. Cell 128, 1063–1076.

Dayma K, Radha V (2011). Cytoskeletal remodeling by C3G to induce neurite-like extensions and inhibit motility in highly invasive breast carcinoma cells. Biochim Biophys Acta 1813, 456–465.

Dayma K, Ramadhas A, Sasikumar K, Radha V (2012). Reciprocal negative regulation between the guanine nucleotide exchange factor C3G and beta-catenin. Genes Cancer 3, 564–577.

Duque-Afonso J, Yalcin A, Berg T, Abdelkarim M, Heidenreich O, Lubbert M (2011). The HDAC class I-specific inhibitor entinostat (MS-275) effectively relieves epigenetic silencing of the LAT2 gene mediated by AML1/ETO. Oncogene 30, 3062–3072.

Fazal F, Minhajuddin M, Bijli KM, McGrath JL, Rahman A (2007). Evidence for actin cytoskeleton-dependent and-independent pathways for RelA/p65 nuclear translocation in endothelial cells. J Biol Chem 282, 3940–3950.

Fernandez V, Jares P, Salaverria I, Gine E, Bea S, Aymerich M, Colomer D, Villamor N, Bosch F, Montserrat E, Campo E (2008). Gene expression profile and genomic changes in disease progression of early-stage chronic lymphocytic leukemia. Haematologica 93, 132–136.

Gama-Carvalho M, Carmo-Fonseca M (2001). The rules and roles of nucleocytoplasmic shuttling proteins. FEBS Lett 498, 157–163.

Gotoh T, Hattori S, Nakamura S, Kitayama H, Noda M, Takai Y, Kaibuchi K, Matsui H, Hatase O, Takahashi H (1995). Identification of Rap1 as a target for the Crk SH3 domain-binding guanine nucleotide-releasing factor C3G. Mol Cell Biol 15, 6746–6753.

Gotoh T, Niino Y, Tokuda M, Hatase O, Nakamura S, Matsuda M, Hattori S (1997). Activation of R-Ras by Ras-guanine nucleotide-releasing factor. J Biol Chem 272, 18602–18607.

Gottardi CJ, Arpin M, Fanning AS, Louvard D (1996). The junction-associated protein, zonula occludens-1, localizes to the nucleus before the maturation and during the remodeling of cell-cell contacts. Proc Natl Acad Sci USA 93, 10779–10784.

Guerrero C, Fernandez-Medarde A, Rojas JM, Font de Mora J, Esteban LM, Santos E (1998). Transformation suppressor activity of C3G is independent of its CDC25-homology domain. Oncogene 16, 613–624.

Hahn M, Dambacher S, Schotta G (2010). Heterochromatin dysregulation in human diseases. J Appl Physiol 109, 232–242.

Hall MN, Corbett AH, Pavlath GK (2011). Regulation of nucleocytoplasmic transport in skeletal muscle. Curr Top Dev Biol 96, 273–302.

Henderson BR, Eleftheriou A (2000). A comparison of the activity, sequence specificity, and CRM1-dependence of different nuclear export signals. Exp Cell Res 256, 213–224.

Hirata T, Nagai H, Koizumi K, Okino K, Harada A, Onda M, Nagahata T, Mikami I, Hirai K, Haraguchi S, *et al.* (2004). Amplification, up-regulation and over-expression of C3G (CRK SH3 domain-binding guanine nucleotide-releasing factor) in non-small cell lung cancers. J Hum Genet 49, 290–295.

Hogan C, Serpente N, Cogram P, Hosking CR, Bialucha CU, Feller SM, Braga VM, Birchmeier W, Fujita Y (2004). Rap1 regulates the formation of E-cadherin-based cell-cell contacts. Mol Cell Biol 24, 6690–6700.

Horton P, Nakai K (1997). Better prediction of protein cellular localization sites with the it k nearest neighbors classifier. Proc Int Conf Intell Syst Mol Biol 5, 147–152.

Hung M-C, Link W (2011). Protein localization in disease and therapy. J Cell Sci 124, 3381–3392.

Ichiba T, Hashimoto Y, Nakaya M, Kuraishi Y, Tanaka S, Kurata T, Mochizuki N, Matsuda M (1999). Activation of C3G guanine nucleotide exchange factor for Rap1 by phosphorylation of tyrosine 504. J Biol Chem 274, 14376–14381.

Ichiba T, Kuraishi Y, Sakai O, Nagata S, Groffen J, Kurata T, Hattori S, Matsuda M (1997). Enhancement of guanine-nucleotide exchange activity of C3G for Rap1 by the expression of Crk, CrkL, and Grb2. J Biol Chem 272, 22215–22220.

Jamieson C, Sharma M, Henderson BR (2011). Regulation of beta-catenin nuclear dynamics by GSK-3beta involves a LEF-1 positive feedback loop. Traffic 12, 16.

Klose RJ, Yan Q, Tothova Z, Yamane K, Erdjument-Bromage H, Tempst P, Gilliland DG, Zhang Y, Kaelin WG Jr (2007). The retinoblastoma binding protein RBP2 is an H3K4 demethylase. Cell 128, 889–900.

Knight JD, Kothary R (2011). The myogenic kinome: protein kinases critical to mammalian skeletal myogenesis. Skelet Muscle 1, 1.

Knudsen BS, Feller SM, Hanafusa H (1994). Four proline-rich sequences of the guanine-nucleotide exchange factor C3G bind with unique specificity to the first Src homology 3 domain of Crk. J Biol Chem 269, 32781–32787.
Kudo N, Matsumori N, Taoka H, Fujiwara D, Schreiner EP, Wolff B, Yoshida M, Horinouchi S (1999). Leptomycin B inactivates CRM1/exportin 1 by covalent modification at a cysteine residue in the central conserved region. Proc Natl Acad Sci USA 96, 9112–9117.
Kumar KS, Ramadhas A, Nayak S, Kaniyappan S, Dayma K, Radha V (2015). C3G (RapGEF1), a regulator of actin dynamics promotes survival and myogenic differentiation of mouse mesenchymal cells. Biochim Biophys Acta 1853, 2629–2639.
Kuret J, Bell H, Cohen P (1986). Identification of high levels of protein phosphatase-1 in rat liver nuclei. FEBS Lett 203, 197–202.
La Cour T, Kiemer L, Mølgaard A, Gupta R, Skriver K, Brunak S (2004). Analysis and prediction of leucine-rich nuclear export signals. Protein Eng Des Sel 17, 527–536.
Lange A, Mills RE, Lange CJ, Stewart M, Devine SE, Corbett AH (2007). Classical nuclear localization signals: definition, function, and interaction with importin α. J Biol Chem 282, 5101–5105.
Londhe P, Davie JK (2013). Interferon-gamma resets muscle cell fate by stimulating the sequential recruitment of JARID2 and PRC2 to promoters to repress myogenesis. Sci Signal 6, ra107.
Marfori M, Mynott A, Ellis JJ, Mehdi AM, Saunders NF, Curmi PM, Forwood JK, Boden M, Kobe B (2011). Molecular basis for specificity of nuclear import and prediction of nuclear localization. Biochim Biophys Acta 1813, 1562–1577.
Martín-Encabo S, Santos E, Guerrero C (2007). C3G mediated suppression of malignant transformation involves activation of PP2A phosphatases at the subcortical actin cytoskeleton. Exp Cell Res 313, 3881–3891.
Martinez-Garcia E, Popovic R, Min DJ, Sweet SM, Thomas PM, Zamdborg L, Heffner A, Will C, Lamy L, Staudt LM, *et al.* (2011). The MMSET histone methyl transferase switches global histone methylation and alters gene expression in t(4;14) multiple myeloma cells. Blood 117, 211–220.
Mattout A, Biran A, Meshorer E (2011). Global epigenetic changes during somatic cell reprogramming to iPS cells. J Mol Cell Biol 3, 341–350.
McEwen AE, Escobar DE, Gottardi CJ (2012). Signaling from the adherens junction. Subcell Biochem 60, 171–196.
Milne TA, Hughes CM, Lloyd R, Yang Z, Rozenblatt-Rosen O, Dou Y, Schnepp RW, Krankel C, LiVolsi VA, Gibbs D (2005). Menin and MLL cooperatively regulate expression of cyclin-dependent kinase inhibitors. Proc Natl Acad Sci USA 102, 749–754.
Mitra A, Kalayarasan S, Gupta V, Radha V (2011). TC-PTP dephosphorylates the guanine nucleotide exchange factor C3G (RapGEF1) and negatively regulates differentiation of human neuroblastoma cells. PLoS One 6, e23681.
Mitra A, Radha V (2010). F-actin-binding domain of c-Abl regulates localized phosphorylation of C3G: role of C3G in c-Abl-mediated cell death. Oncogene 29, 4528–4542.
Mochizuki N, Ohba Y, Kobayashi S, Otsuka N, Graybiel AM, Tanaka S, Matsuda M (2000). Crk activation of JNK via C3G and R-Ras. J Biol Chem 275, 12667–12671.
Moen PT, Johnson CV, Byron M, Shopland LS, Ivana L, Imbalzano AN, Lawrence JB (2004). Repositioning of muscle-specific genes relative to the periphery of SC-35 domains during skeletal myogenesis. Mol Biol Cell 15, 197–206.
Moseley GW, Roth DM, DeJesus MA, Leyton DL, Filmer RP, Pouton CW, Jans DA (2007). Dynein light chain association sequences can facilitate nuclear protein import. Mol Biol Cell 18, 3204–3213.
Nardozzi JD, Lott K, Cingolani G (2010). Phosphorylation meets nuclear import: a review. Cell Commun Signal 8, 32.
Nguyen Ba AN, Pogoutse A, Provart N, Moses AM (2009). NLStradamus: a simple hidden Markov model for nuclear localization signal prediction. BMC Bioinformatics 10, 1.
Ohba Y, Ikuta K, Ogura A, Matsuda J, Mochizuki N, Nagashima K, Kurokawa K, Mayer BJ, Maki K, Miyazaki J, Matsuda M (2001). Requirement for C3G-dependent Rap1 activation for cell adhesion and embryogenesis. EMBO J 20, 3333–3341.
Okino K, Nagai H, Nakayama H, Yoneyama K, Konishi H, Takeshita T (2006). Inactivation of Crk SH3 domain-binding guanine nucleotide-releasing factor (C3G) in cervical squamous cell carcinoma. Int J Gynecol Cancer 16, 763–771.
Otto AM, Paddenberg R, Schubert S, Mannherz HG (1996). Cell-cycle arrest, micronucleus formation, and cell death in growth inhibition of MCF-7 breast cancer cells by tamoxifen and cisplatin. J Cancer Res Clin Oncol 122, 603–612.
Pemberton LF, Paschal BM (2005). Mechanisms of receptor-mediated nuclear import and nuclear export. Traffic 6, 187–198.
Peters AH, Mermoud JE, O'Carroll D, Pagani M, Schweizer D, Brockdorff N, Jenuwein T (2002). Histone H3 lysine 9 methylation is an epigenetic imprint of facultative heterochromatin. Nat Genet 30, 77–80.
Radha V, Mitra A, Dayma K, Sasikumar K (2011). Signalling to actin: role of C3G, a multitasking guanine-nucleotide-exchange factor. Biosci Rep 31, 231–244.
Radha V, Nambirajan S, Swarup G (1994). Subcellular localization of a protein-tyrosine phosphatase: evidence for association with chromatin. Biochem J 299, 41–47.
Radha V, Rajanna A, Gupta RK, Dayma K, Raman T (2008). The guanine nucleotide exchange factor, C3G regulates differentiation and survival of human neuroblastoma cells. J Neurochem 107, 1424–1435.
Radha V, Rajanna A, Mitra A, Rangaraj N, Swarup G (2007). C3G is required for c-Abl-induced filopodia and its overexpression promotes filopodia formation. Exp Cell Res 313, 2476–2492.
Radha V, Rajanna A, Swarup G (2004). Phosphorylated guanine nucleotide exchange factor C3G, induced by pervanadate and Src family kinases localizes to the Golgi and subcortical actin cytoskeleton. BMC Cell Biol 5, 31.
Roth DM, Moseley GW, Glover D, Pouton CW, Jans DA (2007). A microtubule-facilitated nuclear import pathway for cancer regulatory proteins. Traffic 8, 673–686.
Schmitt JM, Stork PJ (2002). PKA phosphorylation of Src mediates cAMP's inhibition of cell growth via Rap1. Mol Cell 9, 85–94.
Shivakrupa R, Radha V, Sudhakar C, Swarup G (2003). Physical and functional interaction between Hck tyrosine kinase and guanine nucleotide exchange factor C3G results in apoptosis, which is independent of C3G catalytic domain. J Biol Chem 278, 52188–52194.
Stambolic V, Ruel L, Woodgett JR (1996). Lithium inhibits glycogen synthase kinase-3 activity and mimics wingless signalling in intact cells. Curr Biol 6, 1664–1669.
Suárez-Sánchez R, Aguilar A, Wagstaff K, Velez G, Azuara-Medina P, Gomez P, Vásquez-Limeta A, Hernández-Hernández O, Lieu K, Jans D (2014). Nucleocytoplasmic shuttling of the Duchenne muscular dystrophy gene product dystrophin Dp71d is dependent on the importin α/β and CRM1 nuclear transporters and microtubule motor dynein. Biochim Biophys Acta 1843, 985–1001.
Tanaka S, Morishita T, Hashimoto Y, Hattori S, Nakamura S, Shibuya M, Matuoka K, Takenawa T, Kurata T, Nagashima K, *et al.* (1994). C3G, a guanine nucleotide-releasing protein expressed ubiquitously, binds to the Src homology 3 domains of CRK and GRB2/ASH proteins. Proc Natl Acad Sci USA 91, 3443–3447.
Utreras E, Henriquez D, Contreras-Vallejos E, Olmos C, Di Genova A, Maass A, Kulkarni AB, Gonzalez-Billault C (2013). Cdk5 regulates Rap1 activity. Neurochem Int 62, 848–853.
Wang Z, Zang C, Rosenfeld JA, Schones DE, Barski A, Cuddapah S, Cui K, Roh T-Y, Peng W, Zhang MQ (2008). Combinatorial patterns of histone acetylations and methylations in the human genome. Nat Genetics 40, 897–903.
Wend P, Fang L, Zhu Q, Schipper JH, Loddenkemper C, Kosel F, Brinkmann V, Eckert K, Hindersin S, Holland JD (2013). Wnt/β-catenin signalling induces MLL to create epigenetic changes in salivary gland tumours. EMBO J 32, 1977–1989.
Wolff B, Sanglier J-J, Wang Y (1997). Leptomycin B is an inhibitor of nuclear export: inhibition of nucleo-cytoplasmic translocation of the human immunodeficiency virus type 1 (HIV-1) Rev protein and Rev-dependent mRNA. Chem Biol 4, 139–147.
Xu L, Massague J (2004). Nucleocytoplasmic shuttling of signal transducers. Nat Rev Mol Cell Biol 5, 209–219.
Zhu J, Nozell S, Wang J, Jiang J, Zhou W, Chen X (2001). p73 cooperates with DNA damage agents to induce apoptosis in MCF7 cells in a p53-dependent manner. Oncogene 20, 4050–4057.